Advanced glycation end products of human β₂ glycoprotein I modulate the maturation and function of DCs

Brigitta Buttari,[1] Elisabetta Profumo,[1] Antonella Capozzi,[2] Francesco Facchiano,[3] Luciano Saso,[4] Maurizio Sorice,[2] and Rachele Riganò[1]

[1]Department of Infectious, Parasitic and Immune-mediated Diseases, Istituto Superiore di Sanità, Rome, Italy; [2]Department of Experimental Medicine, Sapienza University of Rome, Rome, Italy; [3]Department of Hematology, Oncology and Molecular Medicine, Istituto Superiore di Sanità, Rome, Italy; [4]Department of Physiology and Pharmacology "Vittorio Erspamer," Sapienza University of Rome, Rome, Italy

In chronic disorders related to endothelial cell dysfunction, plasma β₂ glycoprotein I (β₂GPI) plays a role as a target antigen of pathogenetic autoimmune responses. However, information is still lacking to clarify why β₂GPI triggers autoimmunity. It is possible that posttranslational modification of the protein, such as nonenzymatic glycosylation, leads to the formation of advanced glycation end products (AGEs). The aim of our study was to explore whether glucose-modified β₂GPI is able to interact and activate monocyte-derived immature dendritic cells (iDCs) from healthy human donors. SDS-PAGE and spectrofluorometric analyses indicated that β₂GPI incubated with glucose was sugar modified, and that this modification likely consisted of AGE formation, resulting in AGE-β₂GPI. AGE-β₂GPI caused phenotypical and functional maturation of iDCs involving the activation of p38 MAPK, ERK, and NF-κB. It also induced on DCs a significant up-regulation of RAGE, the receptor for AGEs. Evidence for RAGE involvement comes from blocking experiments with an anti-RAGE mAb, confocal analysis, and coimmunoprecipitation experiments. AGE-β₂GPI–stimulated DCs had increased allostimulatory ability and primed naive T lymphocytes toward a Th2 polarization. These findings might explain in part the interactive role of β₂GPI, AGEs, and DCs in chronic disorders related to endothelial cell dysfunction. (*Blood*. 2011;117(23):6152-6161)

Introduction

β₂ Glycoprotein I (β₂GPI) or apolipoprotein H is an abundant plasma glycoprotein that binds to negatively charged phospholipids and is involved in clotting mechanisms and lipid pathways.[1] Studies performed in healthy individuals have shown a correlation between plasma β₂GPI and fasting glucose, lipids, and lipoprotein levels.[2] β₂GPI plasma concentrations are strongly associated with the metabolic syndrome and cardiovascular disease in type 2 diabetic patients and could be considered as a clinical marker of cardiovascular risk.[3] This glycoprotein is also the most common target for antiphospholipid antibodies frequently associated with vascular cell dysfunction,[4] thrombotic events, and pro-atherogenic mechanisms.[5-8] In chronic disorders related to endothelial cell dysfunction, such as systemic lupus erythematosus, antiphospholipid antibody syndrome (APS), and atherosclerosis, β₂GPI plays a role as a target antigen for an immune-mediated attack, possibly influencing the progression of disease.[9-13] β₂GPI stimulates a vigorous adaptive humoral response, but also a cellular immune response.[14-15] Cellular immunity to β₂GPI exists in patients with APS[14] and in healthy individuals.[16] Recently, we showed that β₂GPI is a T-cell target in patients with advanced carotid atherosclerotic plaques.[17] Although much is known about β₂GPI as a cofactor in autoimmune diseases, crucial information is still lacking to clarify why this abundant self-plasma protein is the target of autoimmune responses.

The molecular structure and location of the major epitopic region(s) on the β₂GPI molecule are controversial. Several studies have investigated whether the immune response is directed to native β₂GPI[8,9,18] or to cryptic or neoepitopes.[10,13] Decisive events generating cryptic or neoepitopes include β₂GPI binding to anionic surfaces such as phospholipids and oxidative modifications that alter phospholipid binding.[19-22] In a previous study, we revealed the effects of oxidative stress on β₂GPI structure and how this event renders this self-protein able to activate dendritic cells (DCs), the professional antigen-presenting cells capable of activating both innate and adaptive immunity.[23,24] Many other mechanisms may be responsible for generating cryptic structures, and multiple mechanisms receive support from the heterogeneous antigenic specificities in β₂GPI-specific antibodies and T cells. One candidate mechanism is nonenzymatic glycosylation (glycation), a process that leads to the formation of early, intermediate, and advanced glycation end products (AGEs), which are able to modify self-molecule structures and functions. Even though glycation is present physiologically and is modulated by several factors, disorders of glucose metabolism and systemic autoimmune diseases associated with inflammation and oxidative stress may favor the formation and accumulation of these products.[25-27] AGEs accumulate continuously on abundant and long-lived proteins in the extracellular matrix and are present in inflamed tissues such as rheumatoid synovia and atherosclerotic blood vessels.[28,29] Six receptors that recognize and bind AGEs have been identified.[30,31] The best characterized and most extensively studied receptor for AGEs is RAGE, a 46-kDa protein that is mainly expressed on the surface of endothelial cells, on smooth muscle cells, and on monocyte-derived DCs.[32,33] Although there is accumulating evidence that AGEs are involved in the progression of inflammatory and immune-mediated diseases,[29,34,35] further investigations are needed

to clarify the role of glycation in rendering self-proteins able to activate the immune response.

Our objective in this study was to explore possible modifications of β2GPI induced by in vitro exposure to glucose and the effects of the interaction between glucose-modified β2GPI (G-β2GPI) and DCs. We used immunochemical and cytofluorimetric analyses to investigate whether G-β2GPI is able to activate monocyte-derived immature DCs (iDCs) from healthy human donors. We also sought to determine the contribution of RAGE and the signaling molecules downstream of its activation.

Methods

The supplemental materials (available on the *Blood* Web site; see the Supplemental Materials link at the top of the online article) contain an expanded "Methods" section. The procedures for enrollment and study protocols were fully approved by the institutional review board of the transfusion center at the Sapienza University of Rome, and all patients gave informed consent in accordance with the Declaration of Helsinki.

Reagents

Human native β2GPI was purchased from Calbiochem. Endotoxin contamination in β2GPI preparations, as determined by the quantitative chromogenic limulus amebocyte lysate assay (QCL-1000; BioWhittaker), was < 0.05 EU/mL of protein. For all experiments involving β2GPI, polymyxin B was added to the cell-culture medium at 10 μg/mL, concentration that completely neutralizes the activity of these amounts of lipopolysaccharide (LPS).

To study glucose-induced modification of β2GPI, human β2GPI was dissolved in glycation buffer solution (0.144 g/L KH_2PO_4 and 0.426 g/L Na_2HPO_4), pH 7.4, at a 10 μg/mL final concentration and immediately frozen at −80°C under sterile conditions. A highly purified preparation of human albumin (Sigma-Aldrich) treated with D-glucose or D-mannitol under the same conditions used for β2GPI was used. β2GPI aliquots were incubated in the dark at 37°C for different times (from 0-10 days in sealed vials) with the same concentrations (250mM) of glucose (Sigma-Aldrich) or of the nonreducing sugar mannitol (Sigma-Aldrich) used as an isoosmotic control, as described previously.[36] All chemicals used were of the highest available purity.

Bioinformatic analysis

The sequence of the β2GPI precursor (*Homo sapiens*; accession #NP_000033) was subjected to computer-assisted analysis to predict the presence of glycation sites using an algorithm available online (NetGlycate 1.0 Server, http://www.cbs.dtu.dk/services/NetGlycate/), as described previously.[37] The β2GPI sequence was also subjected to PROSITE (http://www.expasy.ch/tools/scanprosite/) and ASC analyses (http://bioinformatic-a.isa.cnr.it/ASC, release 2010), according to a published protocol[38] to evaluate whether one of the predicted glycation sites was located close to functional sites.

Characterization of glucose-dependent modification of β2GPI

SDS-PAGE analysis.　Aliquots (10 μg) of glucose-treated β2GPI (G-β2GPI), mannitol-treated β2GPI (M-β2GPI), and native β2GPI were subjected to SDS-PAGE using 2%-15% acrylamide gradient gels, as described previously.[39] The highly purified preparation of human albumin (Sigma-Aldrich) treated with glucose or mannitol under the same conditions used for β2GPI was used as a positive control. Nonspecific binding of glycated proteins was minimized by saturation of plastic surfaces and checking the protein recovery after each manipulation. The protein molecular weight standards were from Novex® Sharp Pre-Stained Protein Standard (Invitrogen).

Nontryptophan fluorescence studies.　Fluorescence studies were carried out as described previously.[40] β2GPI (20 μg/200 μL final volume in glycation buffer) was incubated at 37°C in the presence or in the absence of glucose or mannitol for 10 days in the dark, and steady-state fluorescence emission spectra were collected with a FluoroMax-2 spectrofluorometer (Jobin Yvon-SPEX) equipped with a thermostated cuvette holder using an excitation wavelength of 370 nm, equal bandwidths for excitation and emission (5/5), 1-second integration time, and data collection between 400 and 600 nm at 20°C. Emission spectra of sugar-incubated β2GPI were obtained by subtracting the contributions of separate identical sugar solutions from the fluorescence of the sugar-β2GPI mixture.

Dot-blot assay

G-β2GPI, M-β2GPI, or native β2GPI (0.5 μg) were spotted onto Immobilon-P strips. Each strip was exposed overnight to serum (diluted 1:100) obtained from 10 patients with primary APS or from 10 control healthy subjects at room temperature. Bound Abs were visualized with HRP-conjugated anti–human IgG, and immunoreactivity was assessed by the chemiluminescence reaction using the ECL system (Amersham).

Generation of DCs and T lymphocytes

Blood samples from 5 healthy blood donors from the transfusion center at the Sapienza University of Rome were used to obtain PBMCs.

Monocytes and iDCs were obtained from PBMCs as described previously.[23] Immature DCs were stimulated with 200 ng/mL of LPS (strain 0111:B4 *Escherichia coli*; Sigma-Aldrich) for 18 hours to obtain LPS-matured DCs. The purity of iDCs was > 95%, as assessed by flow cytometric analysis (FACSCanto using FACSDiva; BD Biosciences) of cells stained with a mixture of CD14-FITC and CD1a-PE mAbs (Pharmingen). $CD4^+$ T cells and untouched $CD4^+$ naive T cells were purified from PBMCs by magnetic selection using anti-$CD4^+$ microbeads and the naive CD4 T-cell isolation kit II (Miltenyi Biotec), according to the manufacturer's instructions. The purity of positively selected $CD4^+$ T cells and negatively selected naive $CD4^+$ T cells was > 95%, as assessed by flow cytometric analysis.

Flow cytometric analysis of phenotypic DC maturation

Preliminary dose-response experiments (0-20 μg/mL) established that G-β2GPI effects were dose dependent, and we chose 10 μg/mL as the optimal reagent concentration for DC stimulation. Five-day human iDCs were stimulated or not with G-β2GPI, M-β2GPI, glucose (5mM), mannitol (5mM), or LPS (200 ng/mL) in the presence or absence of a pretitrated concentration of anti-RAGE (25 μg/mL; Chemicon International) for different times (0-72 hours), then collected and washed. For phenotypic analysis, DCs were stained with PE-conjugated mAbs to CD1a, CD80, and human leukocyte antigen-D region related (HLA-DR), and FITC-conjugated mAbs to CD83, CD86, and CD40 (Pharmingen) and with the mouse anti–human RAGE mAb (Chemicon International) or with isotype-matched control mAb for 30 minutes at 4°C. To assess RAGE surface expression, cells were washed and stained with FITC-conjugated goat anti–mouse Ab (Sigma-Aldrich) for 30 minutes on ice. All samples were analyzed by flow cytometry on a FACSCanto using FACSDiva software (BD Biosciences).

Cytokine production

DC culture supernatants were collected at 18 hours after stimulation with G-β2GPI (10 μg/mL), M-β2GPI (10 μg/mL), glucose (5mM), mannitol (5mM), or LPS (0.2 μg/mL) in the presence or in the absence of the anti-RAGE mAb (25 μg/mL). Levels of IL-12 p70, TNF-α, IL-10, IL-1β, and IL-6 were determined by ELISA (OptEIA kits; BD Biosciences) following the manufacturer's instructions. The limits of detection were as

follows: IL-10, TNF-α, and IL-1β: 16 pg/mL; IL-12p70: 7.8 pg/mL; and IL-6: 2.2 pg/mL.

Coimmunoprecipitation of β2GPI and RAGE

Cell-free lysates from DCs were stimulated with G-β2GPI (10μg/mL) or M-β2GPI (10 μg/mL) for 4 hours or left unstimulated and immunoprecipitated with anti-RAGE mAb (Chemicon International). The immunoprecipitates were subjected to 10% SDS-PAGE, followed by Western blot analysis with anti-β2GPI polyclonal Ab (Affinity Biologicals).

DC allostimulatory ability

The allostimulatory ability of stimulated and unstimulated DCs was evaluated in a standard mixed-lymphocyte reaction. Allogeneic T cells (1×10^5 cells/well) were incubated with irradiated DCs for 3 days at different responder-stimulator ratios (1:4-1:64 DCs:T cells) in a 96-well round-bottom plate. On day 2, 0.5 μCi/well of ^{3}H-methyl-thymidine (Amersham) was added to each well for 18 hours at 37°C. Net counts per minute of triplicate cultures were measured.

T-cell priming assay

To find out whether G-β2GPI- and M-β2GPI–treated DCs primed naive T lymphocytes, negatively selected naive allogeneic T cells were cultured with G-β2GPI- or M-β2GPI–treated DCs at a ratio of 20:1. LPS-matured DCs were used as positive control to prime IL-4- or IFN-γ-expressing T cells. Activated T cells were expanded for 10 days with recombinant IL-2 (30 U/mL; Roche Molecular Biochemicals) added on day 5 in a 24-well plate in complete medium to obtain polyclonal T cell lines to be analyzed for cytokine expression by flow cytometry as previously described.[23]

Confocal laser-scanner microscopy analysis

Immature DCs were stimulated with G-β2GPI (10 μg/mL) or M-β2GPI (10 μg/mL) for 4 hours or left unstimulated and successively fixed in 4% formaldehyde in PBS for 30 minutes at 4°C. After washing, cells were incubated for 1 hour with anti-RAGE mAb (Chemicon International) or polyclonal anti-β2GPI Ab (Affinity Biologicals), followed by addition of Texas Red–conjugated anti–goat or FITC-conjugated anti–mouse Abs (Sigma-Aldrich) for 45 minutes. Images were acquired with a scanning confocal microscope (Leica) equipped with an argon ion laser. FITC and Texas Red fluorochromes were excited at 418 and 518 nm, respectively. Images were collected at 512×512 pixels, processed, and filtered to minimize background.

p38 MAPK and ERK assay

The Fast Activated Cell-based ELISA MAPK assay kit was used to monitor p38 and ERK activation according to the manufacturer's recommendations (Active Motif). In brief, iDCs were cultured and seeded in 96-well plates at 5×10^4 cells/well. Cells were stimulated for different times (0-45 minutes) with G-β2GPI (10 μg/mL), M-β2GPI (10 μg/mL), glucose (5mM), mannitol (5mM), LPS (0.2 μg/mL), or phorbol myristate acetate (PMA; 0.2 μg/mL). The number of cells in each well was counted and normalized using the crystal violet solution. The results were expressed as arbitrary units.

To confirm the role of MAPK in G-β2GPI-induced iDC maturation, iDCs were pre-incubated at 37°C for 30 minutes with the MAPK inhibitor PD098059 or SB203580 before using in iDC phenotypical maturation experiments.

NF-κB translocation

The NF-κB (p65 and p50) transcription factor assay kit (Active Motif) was used to monitor NF-κB activation. Unstimulated DCs and DCs stimulated for 45 minutes at 37°C in 5% CO2 with G-β2GPI (10 μg/mL), M-β2GPI (10 μg/mL), glucose (5mM), mannitol (5mM), LPS (0.2 μg/mL), blocking anti-RAGE Ab (Chemicon International), or control Ab (25 μg/mL) were lysed. Protein content was quantified, and activated levels of p65 and p50 subunits were determined in equal amounts of lysates using antibodies directed against the subunits bound to the oligonucleotide containing the NF-κB consensus-binding site. A HeLa cell extract was used as a positive control and NF-κB wild-type and mutated consensus oligonucleotides were used to monitor the specificity of the assay according to the manufacturer's instructions.

Statistical analysis

Mean values and SD were calculated for each variable under study. All statistical procedures were performed using GraphPad Prism software 4.0. Data were tested for Gaussian distribution with the Kolmogorov-Smirnov test. Normal distributed data were analyzed using 1-way ANOVA with a Bonferroni post hoc test to evaluate the statistical significance of intergroup differences in all tested variables. $P < .05$ was considered statistically significant.

Results

Identification of potential glycation sites in the β2GPI primary structure by bioinformatic analysis

The following lysine residues (Figure 1A) have been found to be potentially involved in β2GPI protein glycation: K25, K63, K123, K129, K157, K287, K303, K306, and K336. The signal peptide[1-19] is underlined in the figure. The protein was further subjected to PROSITE and ASC analyses (see "Bioinformatic analysis"), which indicated that the following cysteine residues are likely to be involved in disulfide bond formation and to be responsible for the Sushi domain secondary structure: C23-C66, C51-C79, C84-C124, C110-C137, C142-C188, C174-C200, C205-C248, and C234-C260. This analysis indicated that at least 2 cysteine residues important for Sushi domain formation, C23 and C124, are very close to the lysine residues K25 and K123, which were previously identified as potential glycation sites. This observation strongly supports the hypothesis that glucose exposure under experimental conditions able to induce protein glycation may significantly modify β2GPI structure and function.

Characterization of G-β2GPI

Purified β2GPI preparations, incubated with glucose or mannitol, were characterized to evaluate the generation of glycoxidation products of the protein. Using SDS-PAGE analysis under denaturing conditions, we determined the presence of the native β2GPI and of a higher–molecular weight complex likely corresponding to the formation of β2GPI dimers in both G-β2GPI and M-β2GPI (Figure 1B panel *i*). Protein dimers can be generated by protein oxidation in culture medium, as described previously.[23] In addition to these forms, in the G-β2GPI, we detected an additional component with a lower mobility than that of the native protein, which was probably caused by sugar molecule addition to β2GPI and resembled the pattern observed for the highly purified preparation of glucose-treated human albumin (Figure 1B panel *ii*) that has been well characterized in previous studies.[39] To confirm the presence of glycation products, protein preparations were further subjected to spectrofluorometric analysis to measure the nontryptophan fluorescence, which represents a known AGE fluorescence marker (Figure 1C). A significant increase of AGE fluorescence was recorded for G-β2GPI compared with M-β2GPI, indicating that human β2GPI under our experimental conditions was sugar modified, and that the modification likely consisted of AGE formation (AGE-β2GPI).

To verify whether the presence of the glycation products may affect sera reactivity with the protein, a dot-blot assay was performed using 10 serum samples from patients with APS. Densitometric analysis showed that the reactivity was stronger for
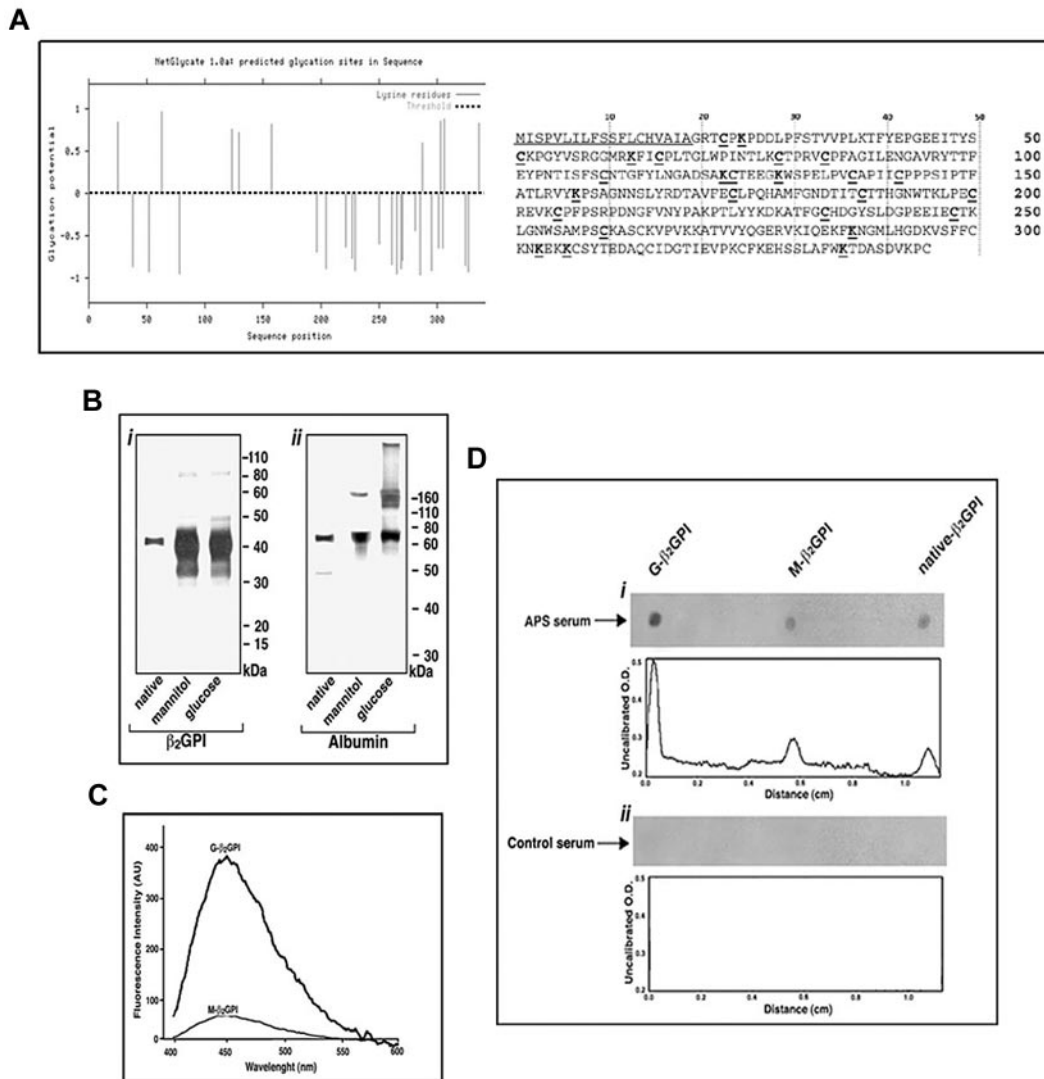
Figure 1. Sugar-induced structural modifications of β₂GPI. (A) Bioinformatic analysis of potential glycation sites within the primary structure of β₂GPI. In the primary structure of human β₂GPI, the underlined sequence represents the signal peptide, the lysine residues (*K*) in bold and underlined indicate the potential glycation sites, and the cysteine residues (*C*) in bold and underlined indicate the residues involved in secondary structure Sushi domain formation. (B) SDS-PAGE analysis of human β₂GPI (left) and human serum albumin (right) incubated for 10 days at 37°C in the presence of 250mM glucose (G-β₂GPI) or mannitol (M-β₂GPI). The results of 1 representative experiment of 3 are shown. (C) Nontryptophan AGE fluorescence of β₂GPI. The emission spectra of G- and M-β₂GPI are reported. The protein was incubated with sugars (250mM) for 10 days at 37°C in the dark (see "Methods"), whereas sugars alone were incubated in separate tubes under the same experimental conditions. At the end of the incubation, the spectra were collected at an excitation of 370 nm, and the reported traces show the fluorescence emission after subtraction of the fluorescence due to the sugars alone. The results of 1 representative experiment of 3 are shown. (D) Dot-blot analysis of β₂GPI preparations. G-β₂GPI, M-β₂GPI, or native β₂GPI (0.5 μg) were spotted onto Immobilon-P strips. Each strip was exposed overnight to serum obtained from patients with APS or from control healthy subjects (diluted 1:100) at room temperature. Bound Abs were visualized with HRP-conjugated anti–human IgG and immunoreactivity was assessed by ECL. Densitometric analysis was performed using ImageJ version 1.43 software. The results of 1 representative experiment of 10 are shown.

G-β₂GPI than for M-β₂GPI or native β₂GPI at the same protein concentration (Figure 1D). None of the healthy subjects' sera reacted with the β₂GPI preparations.

DC maturation and RAGE expression in response to G-β₂GPI

Unstimulated DCs showed an immature phenotype (HLA-DR^low and CD83⁻) and were weakly immunoreactive for CD80, CD86, CD40, and RAGE. As expected, after 18 hours of incubation, LPS caused DCs to mature so that CD83 appeared and HLA-DR, CD80, CD86, and CD40 expression increased. RAGE expression on the DC surface remained unchanged (Figure 2A). Similarly to LPS, G-β₂GPI and M-β₂GPI, but not control sugar, induced DC maturation. Only G-β₂GPI induced a statistically significant up-regulation of RAGE (Figure 2A), and its expression remained

elevated until 72 hours ($P < .01$; Figure 2B). Pretreatment of iDCs with a saturating concentration of the blocking anti-RAGE mAb prevented the appearance of CD83 and the up-regulation of CD86, CD40, and RAGE in response to G-β₂GPI ($P = .01$; Figure 2), but not in response to M-β₂GPI (Figure 2). The anti-RAGE mAb treatment did not affect cell viability, as assessed by trypan blue staining (data not shown). Cell treatment with an equal concentration of irrelevant control Ab did not affect β₂GPI-induced DC maturation (data not shown).

Cytokine production of DCs stimulated with G-β₂GPI

After 18 hours of culture, G-β₂GPI and M-β₂GPI triggered statistically significant up-regulation of IL-12p70, TNF-α, IL-10, and IL-1β secretion (Figure 3). G-β₂GPI–stimulated DCs produced
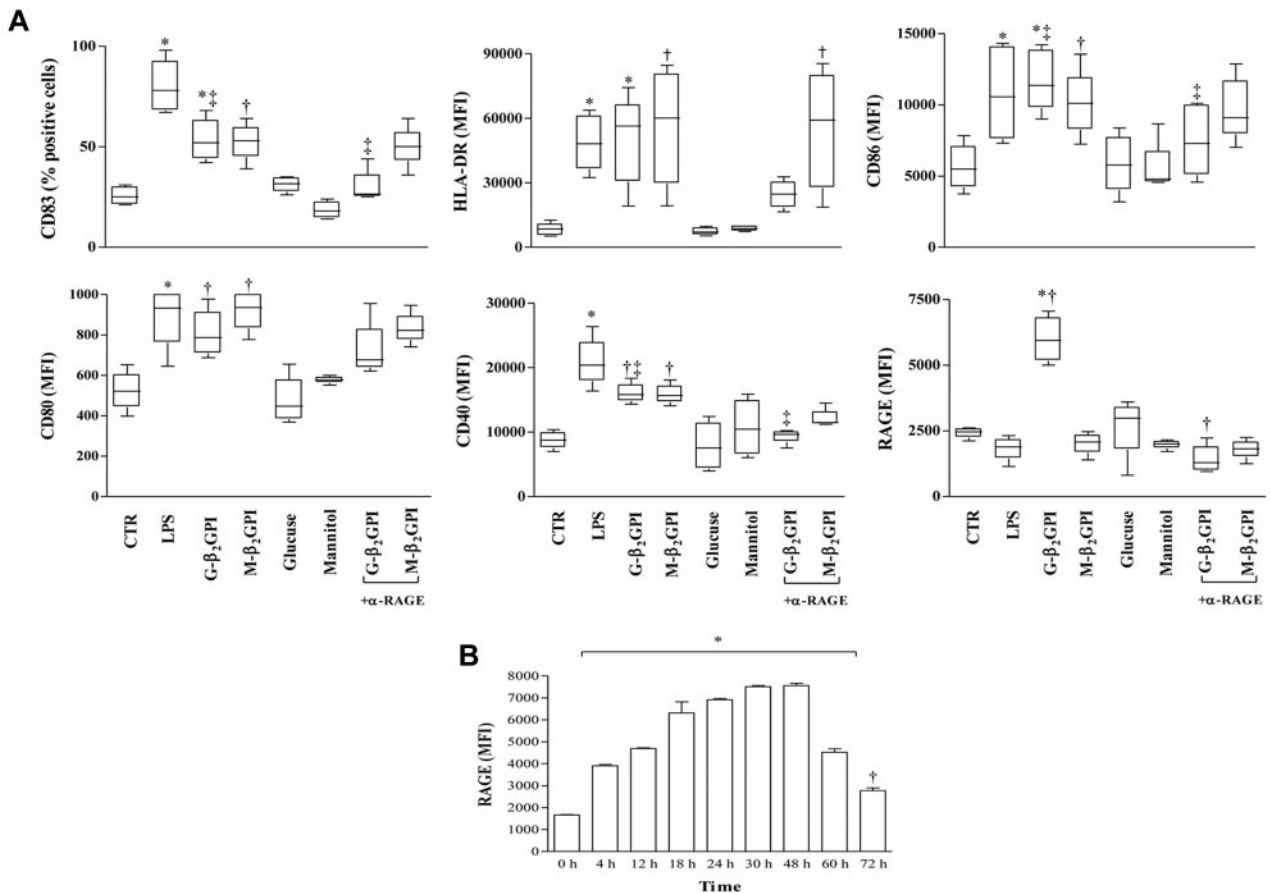
Figure 2. Flow cytometric analysis of phenotypic DC maturation and RAGE expression on immature iDCs stimulated with G-β₂GPI. (A) Flow cytometric analysis of phenotypic DC maturation. After 18 hours of incubation, G-β₂GPI and M-β₂GPI induced similar DC maturation, whereas G-β₂GPI only induced statistically significant up-regulation of RAGE. For HLA-DR: *$P < .01$ and †$P < .001$; for CD83 and CD86: *$P < .001$, †$P < .01$, and ‡$P < .01$ comparing G-β₂GPI vs α-RAGE + G-β₂GPI; for CD80: *$P < .05$ and †$P < .01$; for CD40: *$P < .001$, †$P < .05$, and ‡$P < .05$ comparing G-β₂GPI vs α-RAGE + G-β₂GPI; for RAGE: *$P < .001$ and †$P < .001$ comparing G-β₂GPI vs α-RAGE + G-β₂GPI. (B) Flow cytometric analysis of RAGE expression on iDCs stimulated with G-β₂GPI at different time points. G-β₂GPI induced statistically significant up-regulation of RAGE expression that remained elevated until 72 hours. *$P < .001$ and †$P < .05$.

higher amounts of IL-1β than did M-β₂GPI–stimulated DCs ($P < .001$). Unbound glucose left the up-regulation of cytokine secretion unmodified. Pretreatment of iDCs with saturating concentrations of the blocking anti-RAGE mAb prevented the up-regulation of all cytokines in response to G-β₂GPI ($P = .01$), but not in response to M-β₂GPI (Figure 3).

Allostimulatory ability of DCs stimulated with G-β₂GPI and T-cell priming

When irradiated DCs that had been prestimulated with G-β₂GPI or M-β₂GPI were tested in a mixed-lymphocyte reaction, the relatively low proliferative ability (mean counts per minute) of resting allogenic T cells achievable with unstimulated DCs significantly increased, starting from a DC:T-cell ratio of 1:4 (DC:T-cell ratio of 1:16: unstimulated vs G-β₂GPI, $P = .004$; unstimulated vs M-β₂GPI, $P = .04$) (Figure 4A).

In cell-culture experiments designed to determine whether G-β₂GPI–treated iDCs primed and polarized allogeneic naive CD4$^+$CD45RA$^+$ into typical Th1 or Th2 cells, cytofluorimetric analysis showed that most naive T cells cocultured with G-β₂GPI–treated iDCs turned into typical IL-4–producing Th2 cells (17%). Only a small percentage (4%) differentiated into IFN-γ–producing Th1 cells (Figure 4B). Conversely, control iDCs stimulated with LPS and M-β₂GPI–treated iDCs showed a larger number of IFN-γ–
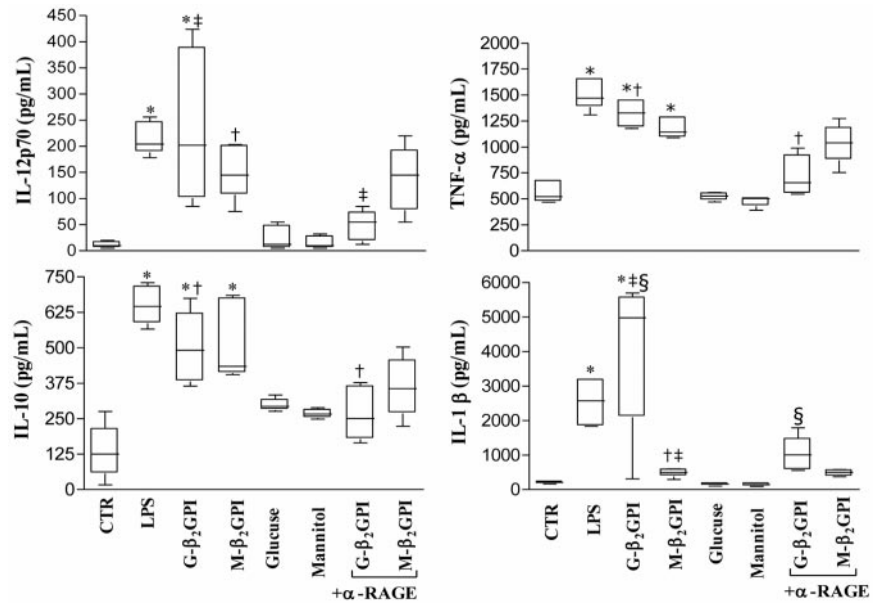
producing T cells and a smaller number of IL-4–producing cells than unstimulated iDCs (Figure 4B).

The bias toward a Th2 polarization after stimulation with G-β₂GPI–treated iDCs was supported by dose-dependent IL-6 production that was higher in culture supernatants from G-β2GPI–treated iDCs than in those from control iDCs (at 10 and 30 μg/mL: $P < .001$) (Figure 4C) and from M-β2GPI–treated iDCs (at 30 μg/mL: $P < .001$). G-β2GPI–treated iDCs also showed a dose-dependent increase of the regulatory cytokine IL-10 levels ($P < .001$) (Figure 4C).

Association and interaction of β₂GPI with RAGE on iDCs

To define the involvement of RAGE in the β₂GPI–iDC interaction, double-immunofluorescence labeling using confocal laser-scanning microscopy was performed on unstimulated and 4-hour–stimulated iDCs. Microscopic analysis demonstrated low expression levels of β₂GPI and RAGE in unstimulated iDCs and M-β2GPI–stimulated DCs (Figure 5A panels *i* and *ii*) and a very low antigen colocalization. Conversely, G-β2GPI–stimulated iDCs were highly positive for both β₂GPI and RAGE, and a colocalization of β₂GPI with RAGE was detected, as revealed in the merged images (Figure 5A panels *iii* and *iv*). Specificity of the Ab reaction was confirmed by the absence of staining in the background controls (supplemental Figure 1).

Figure 3. Cytokine production in β_2GPI–stimulated DC culture supernatants. Five-day human DCs were stimulated with LPS (100 ng/mL), G-β_2GPI (10 μg/mL), M-β_2GPI (10 μg/mL), glucose (250mM), or mannitol (250mM), in the presence or absence of the anti-RAGE mAb (25 μg/mL). Supernatants were collected after 18 hours to measure IL-12 p70, TNF-α, IL-10, and IL-1β by specific ELISA experiments. G-β_2GPI and M-β_2GPI triggered statistically significant up-regulation of all cytokine secretion. Pretreatment of iDCs with saturating concentrations of the blocking anti-RAGE mAb prevented the up-regulation of all cytokines tested in response to G-β_2GPI. For IL-12p70: *$P < .001$, †$P < .05$, and ‡$P < .01$ comparing G-β_2GPI vs α-RAGE + G-β_2GPI; for TNF-α and IL-10: *$P < .001$ and †$P < .001$ comparing G-β_2GPI vs α-RAGE + G-β_2GPI; for IL-1β: *$P < .001$, †$P < .05$, and ‡$P < .001$ comparing G-β_2GPI vs M-β_2GPI and §$P < .001$ comparing G-β_2GPI vs α-RAGE + G-β_2GPI.

β_2GPI-RAGE interaction was confirmed by coimmunoprecipitation experiments. Cells were incubated with G-β_2GPI or M-β_2GPI and immunoprecipitated with anti-RAGE mAb. Western blot analysis of the immunoprecipitates showed a strict interaction between β_2GPI and RAGE, which was higher in G-β2GPI–stimulated iDCs than in M-β2GPI–stimulated iDCs (Figure 5B). The identity of the RAGE bands was confirmed by Western blot analysis (data not shown).

MAPK and NF-κB activation in response to G-β_2GPI

We examined the role of p38 MAPK and ERK activation in G-β2GPI–stimulated iDCs. Increased phosphorylation of p38 and ERK, which peaked at 30 minutes, was observed in G-β2GPI–stimulated DCs (n = 6, $P = .001$; Figure 6A). Glucose control sugar induced a significant activation of ERK ($P = .001$; Figure 6A, panel ii). Pretreatment of cells with the p38 MAPK inhibitor
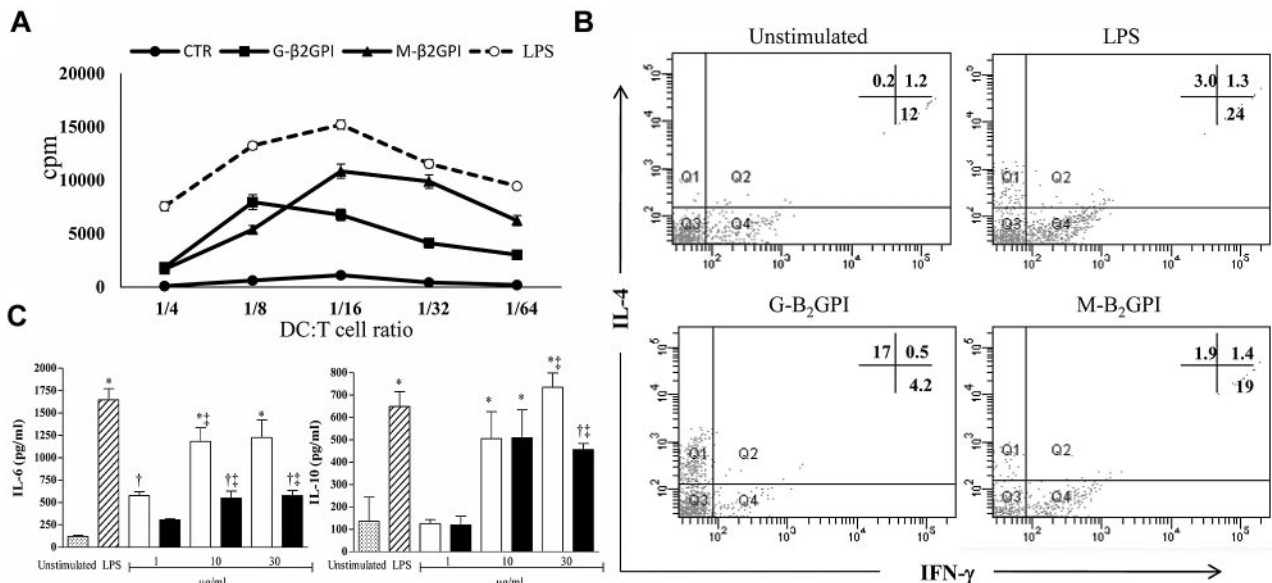

Figure 4. Allostimulatory ability of DCs stimulated with G-β_2GPI and T-cell priming. (A) Irradiated DCs prestimulated with G-β_2GPI, M-β_2GPI, or LPS increased the proliferative ability (mean counts per minute, cpm) of resting allogenic T cells compared with unstimulated DCs. At a DC:T-cell ratio of 1:16, unstimulated DCs vs G-β_2GPI, $P = .004$, and unstimulated DCs vs M-β_2GPI, $P = .04$. (B) G-β_2GPI–treated DCs stimulated allogeneic naive human T cells to produce IFN-γ and IL-4. Five-day human DCs were stimulated with G-β_2GPI, M-β_2GPI, or LPS, or were left unstimulated for 18 hours. A total of 5×10^4 DCs were used to stimulate 1×10^6 allogeneic naive negatively selected CD4$^+$CD45RA$^+$ T cells. Activated T cells were expanded with recombinant human IL-2 (30 U/mL). On day 10, T-cell lines were stimulated with PMA and ionomycin for 4 hours in the presence of brefeldin A. Cells were stained with anti-hu-CD3PerCP and processed for intracellular labeling with anti-human IFN-γ–FITC and anti-human IL-4–PE. The numbers show the percentage of activated CD3$^+$ cells producing the cytokine. Samples were analyzed on a FACSCanto cytofluorometer using FACSDiva software (BD Biosciences). The results of 1 representative experiment of 3 are shown. (C) Dose-response production of IL-6 and IL-10 in β_2GPI–stimulated DC culture supernatants. Five-day human DCs were stimulated with LPS (100 ng/mL), G-β_2GPI (0-30 μg/mL), or M-β_2GPI (0-30 μg/mL), or were left unstimulated. Supernatants were collected after 18 hours to measure IL-6 and IL-10 by specific ELISA experiments. Results are expressed as means ± SD; n = 3.
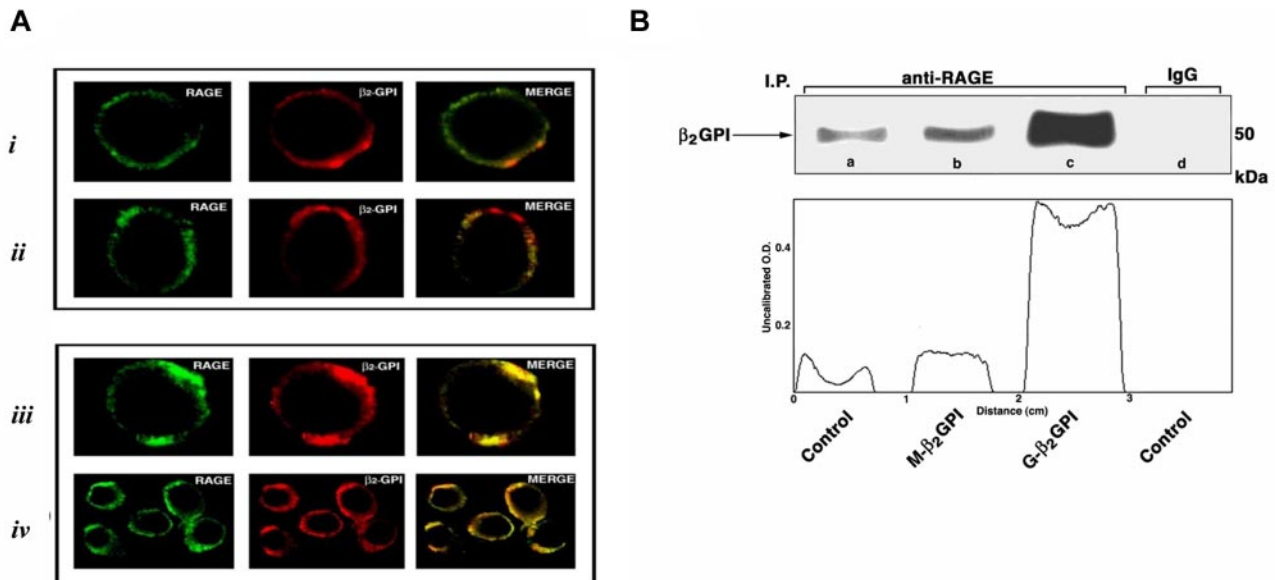
Figure 5. β_2GPI association with RAGE on the iDC surface. (A) Scanning confocal microscopic analysis of β_2GPI association with RAGE on iDC surface. (A) Cells were fixed in 4% formaldehyde in PBS and then labeled with a polyclonal anti-β_2GPI Ab and with a monoclonal anti-RAGE Ab, followed by Texas Red-conjugated anti–goat or FITC-conjugated anti–mouse Ab. Panel *i* shows β_2GPI-RAGE association in untreated (control) cells. One representative cell is shown. Panel *ii* shows β_2GPI-RAGE association in cells treated with M-β_2GPI. One representative cell is shown. Panel *iii* shows β_2GPI-RAGE association in cells treated with G-β_2GPI. One representative cell is shown. Panel *iv* shows β_2GPI-RAGE association in cells treated with G-β_2GPI. A group of cells is shown. (B) Coimmunoprecipitation analysis of β_2GPI association with RAGE on the iDC surface. Cells were incubated with M-β_2GPI or G-β_2GPI and then immunoprecipitated with anti-RAGE mAb. The immunoprecipitates were analyzed by Western blotting using an anti β_2GPI polyclonal Ab. Lane a shows the reactivity of anti-β_2GPI with RAGE immunoprecipitate from untreated cells. Lane b shows the reactivity of anti-β_2GPI with RAGE immunoprecipitate from M-β_2GPI–stimulated cells. Lane c shows the reactivity of anti-β_2GPI with RAGE immunoprecipitate from G-β_2GPI–stimulated cells. Lane d shows the reactivity of anti-β_2GPI with immunoprecipitate with IgG with irrelevant specificity from untreated cells.

SB203580 prevented the phenotypic maturation of DCs (as shown by the appearance of CD83, $P < .05$; Figure 6B), and the increase of RAGE expression in response to G-β_2GPI ($P < .001$; Figure 6C), whereas the ERK MAPK inhibitor PD98059 prevented only the increase of RAGE ($P < .001$; Figure 6C).

In G-β_2GPI- and M-β2GPI–stimulated DCs, active p65 and p50 levels were significantly increased compared with iDCs (n = 6, $P \leq .01$ and $P \leq .001$, respectively, Figure 6D). These levels were only slightly lower than those obtained after LPS stimulation (LPS vs medium, $P < .001$). Glucose control sugar did not induce any significant NF-κB activation. Pretreatment of iDCs with saturating concentrations of the blocking anti-RAGE mAb prevented the up-regulation of active p65 in response to G-β_2GPI ($P = .001$; Figure 6D panel *i*), but not to M-β_2GPI. This assay was specific, because incubation of a HeLa extract in the presence of an unbound wild-type consensus oligonucleotide abolished binding of both subunits; conversely, incubation of the HeLa extract with mutated consensus oligonucleotide did not affect NF-κB binding (data not shown).

Discussion

Our in vitro study provides new data showing the formation of an AGE-β_2GPI after in vitro exposure to glucose and the interaction between AGE-β_2GPI and DCs. Our results strongly suggest that AGE-β_2GPI is able to activate monocyte-derived iDCs from healthy donors, underlining the role of glycation in rendering self-proteins such as β_2GPI able to activate the immune response.[25] We have demonstrated that RAGE is engaged by human AGE-β_2GPI and is able to trigger a signaling pathway mediated by the activation of ERK, p38 MAPK, and NF-κB.

In the present study, we primarily investigated the effects of glucose treatment on β_2GPI structural modifications, bearing in mind that in human serum and tissues, many other molecules contribute to the total glycating activity. Furthermore, it is important to take into account that protein glycation is an accumulation effect, and therefore longer incubation with lower concentrations of glycating agents might be comparable to shorter incubations with higher concentrations and vice versa. Therefore, it is expected that longer exposure of β_2GPI may induce more evident structural modifications and production of fluorescent products. In our experiments, we verified the occurrence of glycation in G-β_2GPI by the appearance of high–molecular weight complexes and by the formation of a fluorescent AGE. The presence of β_2GPI dimers in both sugar-treated β_2GPI preparations may have been due to protein oxidation spontaneously occurring in the culture medium, as described previously.[23]

Our bioinformatic analyses of the β_2GPI primary structure indicated that several potential glycation sites are present within the molecule, and at least 2 of them are very close to the cysteine residues essential to determining the secondary structure of β_2GPI, which is characterized by the presence of Sushi domains. Therefore, our structural studies indicate that glucose treatment may induce a significant misfolding effect on the β_2GPI structure, likely leading to expression of cryptic or neo-epitopes recognized by the immune system and to significant functional effects. Indeed, dot-blot experiments showed that glucose treatment may increase patients' sera reactivity with the protein, thus suggesting a possible role for this modified protein in the activation of immune system.

When we analyzed the phenotypic characteristics of DCs, the professional antigen-presenting cells capable of activating the immune response, after stimulation with G-β_2GPI, we found that the mature DC-restricted marker CD83 appeared. In parallel,
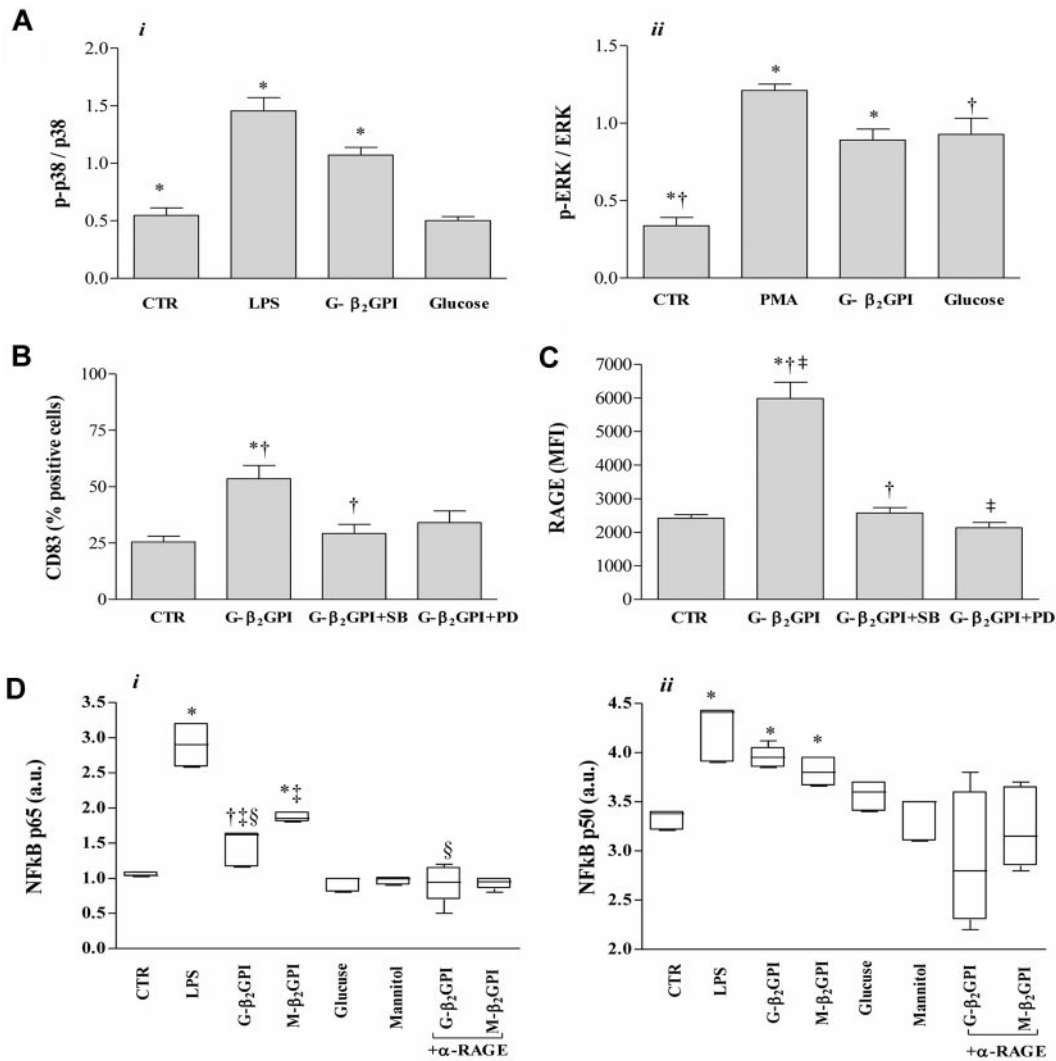
Figure 6. Analysis of MAPK and NK-κB activation and surface molecule expression (CD83, RAGE) in G-β_2GPI-stimulated DCs. (A) p38 MAPK and ERK activation in DCs stimulated with G-β_2GPI. iDCs (5 × 10^4 cells) stimulated for 30 minutes with G-β_2GPI (10 μg/mL), glucose (5mM), LPS (0.2 μg/mL), or PMA (0.2 μg/mL) were analyzed by cell-based ELISA MAPK assay to monitor p38 and ERK activation. The number of cells in each well was counted and normalized using crystal violet solution, and the results are expressed as arbitrary units. G-β_2GPI induced the activation of both the p38 MAPK and the ERK pathways (n = 6, P = .001). (B, C) Flow cytometric analysis of CD83 and RAGE expression in DCs stimulated with G-β_2GPI after pretreatment with specific inhibitors for the MAPK family. The increase in CD83 and RAGE expression after G-β_2GPI stimulation was significantly prevented by pretreatment of iDCs with the p38 MAPK inhibitor SB203580, whereas the pretreatment of iDCs with the ERK inhibitor PD98059 prevented only the up-regulation of RAGE expression (n = 3, CD83: *$P < .01$ and †$P < .05$ comparing G-β_2GPI vs G-β_2GPI + SB; RAGE: *$P < .001$ and †$P < .001$ comparing G-β_2GPI vs G-β_2GPI + SB and ‡$P < .001$ comparing G-β_2GPI vs G-β_2GPI + PD). (D) NF-κB activation in G- and M-β_2GPI–stimulated DCs. In G-β_2GPI- and M-β_2GPI–stimulated DCs, active p65 and p50 levels were significantly increased compared with unstimulated iDCs. Pretreatment of iDCs with saturating concentrations of the blocking anti-RAGE mAb prevented the up-regulation of active p65 in response to G-β_2GPI, but not in response to M-β_2GPI (n = 6, p65: *$P \leq .001$, †$P < .01$, and ‡$P < .001$ comparing G-β_2GPI vs M-β_2GPI and §$P = .001$ comparing G-β_2GPI vs α-RAGE + G-β_2GPI; for p50: *$P \leq .001$).

G-β_2GPI up-regulated the surface molecules HLA-DR, CD80, CD86, and CD40, indicating that G-β_2GPI induced a mature DC phenotype.

Further information on DC activation induced by G-β_2GPI comes from our experiments investigating functional changes in DCs. G-β_2GPI preparations specifically stimulated DCs to secrete IL-12p70, TNF-α, and IL-1β, the cytokines that support the differentiation of Th1 cells[41,42] and form a link between innate and adaptive immunity. G-β_2GPI stimulated DCs to also secrete IL-10 and IL-6, cytokines that promote Th2 responses and inhibit Th1 polarization. In agreement with these results, our data also indicate that G-β_2GPI–stimulated DCs activated a Th2-type response by allogeneic naive T cells, characterized by IL-4 expression. This Th2 bias is consistent with the presence of β_2GPI–autoreactive T cells with a Th2 profile determined in the peripheral blood of

patients with APS[14] and in patients with advanced carotid atherosclerotic plaques.[17]

In addition, G-β_2GPI enhanced the capacity of DCs to stimulate T-cell proliferation in an allogenic mixed-lymphocyte reaction. Further studies will be needed to verify whether protein glycation may modify DC uptake and presentation of β_2GPI, thus inducing T- and B-cell immunogenicity.

It was not surprising that, like G-β_2GPI, M-β_2GPI induced a DC phenotypical and functional maturation. This result is in agreement with our previous findings showing that oxidized β_2GPI generated in the culture medium is able to active DCs.[23]

Information on DC activation specifically induced by AGE-β_2GPI came from our experiments demonstrating that RAGE, the specific receptor for AGEs,[30-32] was overexpressed in DCs treated with AGE-β_2GPI, but not with M-β_2GPI. Receptor binding receives

further support from our preliminary experiments showing that the changes in the percentage of phenotypically mature DCs induced by AGE-β_2GPI were dose dependent. Two different experimental approaches indicated that RAGE up-regulation is a critical event in activating DCs. The first evidence came from experiments showing that pretreatment of iDCs with saturating concentrations of the blocking anti-RAGE mAb induced a significant decrease of DC phenotypic surface-marker expression (CD83, CD86, and CD40) and of cytokine production in response to G-β_2GPI but not to M-β_2GPI. The latter derives from the results of scanning confocal microscopy analysis demonstrating that expression and colocalization of β_2GPI and RAGE were higher in G-β_2GPI–stimulated iDCs than in M-β_2GPI–stimulated iDCs. This finding was confirmed and extended by coimmunoprecipitation experiments revealing a strict interaction between G-β_2GPI and RAGE, which was higher in iDCs stimulated with G-β_2GPI than in those stimulated with M-β_2GPI.

Our findings also help to explain how AGE-β_2GPI may activate DCs. Under our experimental conditions, the interaction with RAGE is involved in the maturative effects of DCs through a signaling cascade implicating the activation of both the p38 MAPK and ERK pathways and NF-κB translocation. Our findings are in agreement with previous evidence demonstrating that AGEs are able to activate both p38 and ERK1/2 MAPK and NF-κB after binding to RAGE,[43] leading to an enhanced inflammatory response and local tissue injury.[33,44] Our study indicates that the inflammatory response mediated by G-β_2GPI–activated DCs is characterized by high IL-1β production, a cytokine linked to several autoinflammatory disorders.[45]

Although enhanced in diabetes, AGE accumulation also occurs in euglycemia, with aging,[46] and in systemic autoimmune diseases,[47] albeit to lower degrees, driven by oxidative stress and inflammation. Because RAGE expression is increased in the inflammatory milieu, and so is present in patients with systemic autoimmune diseases, these patients are especially susceptible to the deleterious effects of AGEs. The AGE-RAGE interaction might act as a proinflammatory loop in these patients, thus contributing to chronic low-grade inflammation and rendering these individuals susceptible to the development of accelerated endothelial dysfunction and atherosclerosis.[48]

Our in vitro findings also help to explain why the abundant plasma protein β_2GPI becomes immunogenic in vivo. Glycation and glycoxidation of β_2GPI can change the protein structure. It is conceivable to suggest that structurally changed β_2GPI, acting as an inflammatory stimulus, is able to activate immunogenic DCs but also to alter tolerogenic DC functions, thus leading to autoreactive T-cell responses and the development of an autoimmune response.[49] It is generally agreed that some autoimmune diseases are associated with abnormal presentation of cryptic or neo-epitopes of self-antigens by DCs. Because epitope dominance is influenced by protein structure,[50] glycation and glycoxidation events may change the molecular context of β_2GPI epitopes (for altered secondary or tertiary structure), thus permitting the efficient presentation of cryptic and neo-determinants.

In conclusion, it can be theorized from our results that a microenvironment predisposes local β_2GPI to glycation and/or oxidation, thereby initiating a local autoimmune process. Chronic oxidative stress causes an accumulation of AGEs. The generation of AGEs and augmentation of proinflammatory mechanisms in the vessel provide a potent feedback loop for sustained oxidant stress, ongoing generation of AGEs, and vascular perturbation. Our in vitro findings now call for studies in patients with chronic disorders related to endothelial cell dysfunction to verify the pathogenetic role of glycated β_2GPI as a trigger of specific humoral and cellular immune reactions. In addition to inhibiting glycation and glycoxidation reactions, antioxidant therapy may also act directly by dismantling AGE/RAGE signaling, thus preventing or reducing the complications of cardiovascular disease.

Acknowledgments

Authorship

Contribution: B.B., E.P., A.C., and F.F performed research; B.B., L.S., F.F., and R.R. designed research and analyzed data; and B.B., M.S., and R.R. designed research and wrote the paper.

Conflict-of-interest disclosure: The authors declare no competing financial interests.

Correspondence: Rachele Riganò, Istituto Superiore di Sanità, Department of Infectious, Parasitic and Immune-mediated Diseases, 299 Viale Regina Elena, Rome, Italy; e-mail: rachele.rigano@iss.it.

References

1. Müller G, Biering A, Lux E, Richter V. Beta-2 glycoprotein I analysis in patients with hyperlipoproteinaemia, arteriosclerotic occlusive disease and diabetes mellitus. *Z Gesamte Inn Med.* 1983;38(10):282-284.

2. Crook M, Chng SI, Lumb P, Reid F. Serum apolipoprotein H and its relationship to blood pressure, serum lipids, fasting plasma glucose and insulin in normal individuals. *Ann Clin Biochem.* 2001;38(pt 5):494-498.

3. Castro A, Lázaro I, Selva DM, et al. APOH is increased in the plasma and liver of type 2 diabetic patients with metabolic syndrome. *Atherosclerosis.* 2010;209(1):201-205.

4. Hattori N, Kuwana M, Kaburaki J, Mimori T, Ikeda Y, Kawakami Y. T cells that are autoreactive to beta2-glycoprotein I in patients with antiphospholipid syndrome and healthy individuals. *Arthritis Rheum.* 2000;43(1):65-75.

5. Levine JS, Branch DW, Rauch J. The antiphospholipid syndrome. *N Engl J Med.* 2002;346(10):752-763.

6. Ferro D, Pittoni V, Quintarelli C, et al. Coexistence of antiphospholipid antibodies and endothelial perturbation in systemic lupus erythematosus patients with ongoing prothrombotic state. *Circulation.* 1997;95(6):1425-1432.

7. George J, Shoenfeld Y, Harats D. The involvement of beta2-glycoprotein I (beta2-GPI) in human and murine atherosclerosis. *J Autoimmun.* 1999;13(1):57-60.

8. García CO, Kanbour-Shakir A, Tang H, Molina JF, Espinoza LR, Gharavi AE. Induction of experimental antiphospholipid antibody syndrome in PL/J mice following immunization with beta2GPI. *Am J Reprod Immunol.* 1997;37(1):118-124.

9. Tincani A, Spatola L, Prati E, et al. The anti-beta2-glycoprotein I activity in human antiphospholipid syndrome sera is due to monoreactive low-affinity autoantibodies directed to epitopes located on native beta2-glycoprotein I and preserved during species' evolution. *J Immunol.* 1996;157(12):5732-5738.

10. Aron AL, Cuellar RL,. Brey RL, Meceown S, Espinoza LR, Shoenfeld Y. Early onset of autoimmunity in MLR/++ mice following immunization with beta2-glycoprotein I. *Clin Exp Immunol.* 1995;101(1):78-82.

11. Shoenfeld Y, Twig G, Katz U, Sherer Y. Autoantibody explosion in antiphospholipid syndrome. *J Autoimmun.* 2008;30(1-2):74-83.

12. Matsuura E, Kobayashi K, Koike T, Shoenfeld Y. Autoantibody-mediated atherosclerosis. *Autoimmun Rev.* 2002;1(6):348-353.

13. Gharavi AE, Summaritano LR, Wen J, Elkon EB. Induction of antiphospholipid antibodies by immunization with beta2-glycoprotein I (apolipoprotein H). *J Clin Invest.* 1992;90(3):1105-1111.

14. Arai T, Yoshida K, Kaburaki J, et al. Autoreactive CD4 (+) T-cell clones to beta2-glycoprotein I in patients with antiphospholipid syndrome: preferential recognition of the major phospholipid-binding site. *Blood.* 2001;98(6):1889-1896.

15. Matsuura E, Igarashi Y, Yasuda T, Triplett DA,

Koike T. Anticardiolipin antibodies recognize beta2-glycoprotein structure altered by interacting with an oxygen modified solid phase surface. *J Exp Med.* 1994;179(2):457-462.

16. Bertolaccini ML, Hughes GR, Khamashta MA. Revisiting antiphospholipid antibodies: from targeting phospholipids to phospholipid binding proteins. *Clin Lab.* 2004;50(11-12):653-665.

17. Profumo E, Buttari B, Alessandri C, et al. Beta2-glycoprotein I is a target of T cell reactivity in patients with advanced carotid atherosclerotic plaques. *Int J Immunopathol Pharmacol.* 2010; 23(1):73-80.

18. Roubey RA, Eisenberg RA, Harper MF, Winfield JB. "Anticardiolipin" autoantibodies recognize beta 2-glycoprotein I in the absence of phospholipid. Importance of Ag density and bivalent binding. *J Immunol.* 1995;154(2):954-960.

19. Wang MX, Kandiah D, Ichikawa K, et al. Epitope specificity of monoclonal anti-beta2-glycoprotein I antibodies derived from patients with the antiphospholipid syndrome. *J Immunol.* 1995;155(3): 1629-1636.

20. Hörkkö S, Miller E, Branch DW, Palinski W, Witztum JL. The epitopes for some antiphospholipid antibodies are adducts of oxidized phospholipid and beta2-glycoprotein 1 (and other proteins). *Proc Natl Acad Sci. U S A.* 1997;94(19): 10356-10361.

21. Matsuura E, Igarashi Y, Fujimoto M, et al. Heterogeneity of anticardiolipin antibodies defined by the anticardiolipin cofactor. *J Immunol.* 1992; 148(12):3885-3891.

22. Arvieux J, Regnault V, Hachulla E, Darnige L, Berthou F, Youinou P. Oxidation of beta2-glycoprotein I (beta2-GPI) by the hydroxil radical alters phospholipid binding and modulates recognition by anti-beta2-GPI autoantibodies. *Thromb Haemost.* 2001;86(4):1070-1076.

23. Buttari B, Profumo E, Mattei V, et al. Oxidized beta2-glycoprotein I induces human dendritic cell maturation and promotes a T helper type 1 response. *Blood.* 2005;106(12):3880-3887.

24. Ueno H, Klechevsky E, Morita R, et al. Dendritic cell subsets in health and disease. *Immunol Rev.* 2007;219:118-142.

25. Ramasamy R, Yan SF, Schmidt AM. RAGE: therapeutic target and biomarker of the inflammatory response–the evidence mounts. *J Leukoc Biol.* 2009;86(3):505-512.

26. Shanmugam N, Kim YS, Lanting L, Natarajan R. Regulation of cyclooxygenase-2 expression in monocytes by ligation of the receptor for ad-

vanced glycation end products. *J Biol Chem.* 2003;278(37):34834-34844.

27. Bierhaus A, Hofmann MA, Ziegler R, Nawroth PP. AGEs and their interaction with AGE-receptors in vascular disease and diabetes mellitus. I. The AGE concept. *Cardiovasc Res.* 1998;37(3):586-600.

28. Basta G, Schmidt AM, De Caterina R. Advanced glycation end products and vascular inflammation: implications for accelerated atherosclerosis in diabetes. *Cardiovasc Res.* 2004;63(4):582-592.

29. Smit AJ, Lutgers HL. The clinical relevance of AGE and recent developments in pharmaceutics to reduce AGE accumulation. *Curr Med Chem.* 2004;11(20):2767-2784.

30. Li YM, Mitsuhashi T, Wojciechowicz D, et al. Molecular identity and cellular distribution of advanced glycation endproduct receptors: relationship of p60 to OST-48 and p90 to 80K-H membrane proteins. *Proc Natl Acad Sci U S A.* 1996;93(20):11047-11052.

31. Miyazaki A, Nakayama H, Horiuchi S. Scavenger receptors that recognize advanced glycation end products. *Trends Cardiovasc Med.* 2002;12(6): 258-262.

32. Brett J, Schmidt AM, Yan SD, et al. Survey of the distribution of a newly characterized receptor for advanced glycation end products in tissues. *Am J Pathol.* 1993;143(6):1699-1712.

33. Ge J, Jia Q, Liang C, et al. Advanced glycosylation end products might promote atherosclerosis through inducing the immune maturation of dendritic cells. *Arterioscler Thromb Vasc Biol.* 2005; 25(10):2157-2163.

34. Cipollone F, Iezzi A, Fazia M, et al. The receptor RAGE as a progression factor amplifying arachidonate-dependent inflammatory and proteolytic response in human atherosclerotic plaques: role of glycemic control. *Circulation.* 2003;108(9): 1070-1077.

35. Schmidt AM, Yan SD, Yan SF, Stern DM. The multiligand receptor RAGE as a progression factor amplifying immune and inflammatory responses. *J Clin Invest.* 2001;108(7):949-955.

36. Facchiano F, D'Arcangelo D, Russo K, et al. Glycated fibroblast growth factor-2 is quickly produced in vitro upon low-millimolar glucose treatment and detected in vivo in diabetic mice. *Mol Endocrinol.* 2006;20(11):2806-2818.

37. Johansen MB, Kiemer L, Brunak S. Analysis and prediction of mammalian protein glycation. *Glycobiology.* 2006;16(9):844-853.

38. Facchiano AM, Facchiano A, Facchiano F. Active Sequences Collection (ASC) database: a new tool to assign functions to protein sequences. *Nucleic Acids Res.* 2003;31(1):379-382.

39. Facchiano F, Lentini A, Fogliano V, et al. Sugar-induced modification of fibroblast growth factor 2 reduces its angiogenic activity in vivo. *Am J Pathol.* 2002;161(2):531-541.

40. Kumar PA, Kumar MS, Reddy GB. Effect of glycation on alpha-crystallin structure and chaperone-like function. *Biochem J.* 2007;408(2):251-258.

41. Geginat J, Sallusto F, Lanzavecchia A. Cytokine-driven proliferation and differentiation of human naive, central memory and effector memory CD4+ T cells. *Pathol Biol.* 2003;51(2):64-66.

42. Ma X, Chow J, Gri G, et al. The interleukin 12 p40 gene promoter is primed by interferon gamma in monocytic cells. *J Exp Med.* 1996;183(1):147-157.

43. Koka V, Wang W, Huang XR, Kim-Mitsuyama S, Truong LD, Lan HY. Advanced glycation end products activate a chymase-dependent angiotensin II-generating pathway in diabetic complications. *Circulation.* 2006;113(10):1353-1360.

44. Herold K, Moser B, Chen Y, et al. Receptor for advanced glycation end products (RAGE) in a dash to the rescue: inflammatory signals gone awry in the primal response to stress. *J Leukoc Biol.* 2007;82(2):204-212.

45. Dinarello CA. Blocking IL-1 in systemic inflammation. *J Exp Med.* 2005;201(9):1355-1359.

46. Yan SF, Ramasamy R, Naka Y, Schmidt AM. Glycation, inflammation, and RAGE: a scaffold for the macrovascular complications of diabetes and beyond. *Circ Res.* 2003;93(12):1159-1169.

47. Nienhuis HL, de Leeuw K, Bijzet J, et al. Skin autofluorescence is increased in systemic lupus erythematosus but is not reflected by elevated plasma levels of AGE. *Rheumatology (Oxford).* 2008;47(10):1554-1558.

48. Nienhuis HL, Westra J, Smit AJ, Limburg PC, Kallenberg CG, Bijl M. AGE and their receptor RAGE in systemic autoimmune diseases: an inflammation propagating factor contributing to accelerated atherosclerosis. *Autoimmunity.* 2009; 42(4):302-304.

49. Torres-Aguilar H, Blank M, Jara LJ, Shoenfeld Y. Tolerogenic dendritic cells in autoimmune diseases: crucial players in induction and prevention of autoimmunity. *Autoimmun Rev.* 2010;10(1):8-17.

50. Moudgil KD, Sercarz EE. Understanding crypticity is the key to revealing the pathogenesis of autoimmunity. *Trends Immunol.* 2005;26(7):355-359.